

Observation of anomalous $\Upsilon(1S)\pi^+\pi^-$ and $\Upsilon(2S)\pi^+\pi^-$ production near the $\Upsilon(5S)$ resonance

K.-F. Chen,²⁵ W.-S. Hou,²⁵ M. Shapkin,¹¹ A. Sokolov,¹¹ I. Adachi,⁸ H. Aihara,⁴⁰ K. Arinstein,¹ V. Aulchenko,¹ T. Aushev,^{17,12} A. M. Bakich,³⁷ V. Balagura,¹² A. Bay,¹⁷ K. Belous,¹¹ V. Bhardwaj,³² U. Bitenc,¹³ A. Bondar,¹ A. Bozek,²⁶ M. Bračko,^{19,13} J. Brodzicka,⁸ T. E. Browder,⁷ P. Chang,²⁵ Y. Chao,²⁵ A. Chen,²³ W. T. Chen,²³ R. Chistov,¹² Y. Choi,³⁶ J. Dalseno,²⁰ M. Danilov,¹² M. Dash,⁴⁴ A. Drutskoy,³ S. Eidelman,¹ N. Gabyshev,¹ B. Golob,^{18,13} H. Ha,¹⁵ J. Haba,⁸ K. Hayasaka,²¹ H. Hayashii,²² M. Hazumi,⁸ D. Heffernan,³¹ Y. Hoshi,³⁹ Y. B. Hsiung,²⁵ H. J. Hyun,¹⁶ T. Iijima,²¹ K. Inami,²¹ A. Ishikawa,³³ H. Ishino,⁴¹ R. Itoh,⁸ M. Iwasaki,⁴⁰ Y. Iwasaki,⁸ D. H. Kah,¹⁶ J. H. Kang,⁴⁵ P. Kapusta,²⁶ N. Katayama,⁸ H. Kawai,² T. Kawasaki,²⁸ H. Kichimi,⁸ H. O. Kim,¹⁶ S. K. Kim,³⁵ Y. J. Kim,⁵ K. Kinoshita,³ S. Korpar,^{19,13} P. Križan,^{18,13} P. Krokovny,⁸ R. Kumar,³² C. C. Kuo,²³ Y.-J. Kwon,⁴⁵ J. S. Lange,⁴ J. S. Lee,³⁶ M. J. Lee,³⁵ T. Lesiak,²⁶ A. Limosani,²⁰ S.-W. Lin,²⁵ Y. Liu,⁵ D. Liventsev,¹² F. Mandl,¹⁰ S. McOnie,³⁷ T. Medvedeva,¹² W. Mitaroff,¹⁰ K. Miyabayashi,²² H. Miyake,³¹ H. Miyata,²⁸ Y. Miyazaki,²¹ R. Mizuk,¹² G. R. Moloney,²⁰ M. Nakao,⁸ Z. Natkaniec,²⁶ S. Nishida,⁸ O. Nitoh,⁴³ S. Ogawa,³⁸ T. Ohshima,²¹ S. Okuno,¹⁴ S. L. Olsen,^{7,9} W. Ostrowicz,²⁶ H. Ozaki,⁸ P. Pakhlov,¹² G. Pakhlova,¹² H. Palka,²⁶ C. W. Park,³⁶ H. Park,¹⁶ K. S. Park,³⁶ R. Pestotnik,¹³ L. E. Piilonen,⁴⁴ Y. Sakai,⁸ O. Schneider,¹⁷ J. Schümann,⁸ C. Schwanda,¹⁰ A. J. Schwartz,³ K. Senyo,²¹ M. E. Sevior,²⁰ C. P. Shen,⁹ H. Shibuya,³⁸ J.-G. Shiu,²⁵ B. Shwartz,¹ A. Somov,³ S. Stanič,²⁹ M. Starič,¹³ T. Sumiyoshi,⁴² F. Takasaki,⁸ K. Tamai,⁸ M. Tanaka,⁸ G. N. Taylor,²⁰ Y. Teramoto,³⁰ K. Trabelsi,⁸ S. Uehara,⁸ K. Ueno,²⁵ T. Uglov,¹² Y. Unno,⁶ S. Uno,⁸ P. Urquijo,²⁰ Y. Ushiroda,⁸ Y. Usov,¹ G. Varner,⁷ K. Vervink,¹⁷ S. Villa,¹⁷ C. C. Wang,²⁵ C. H. Wang,²⁴ M.-Z. Wang,²⁵ P. Wang,⁹ X. L. Wang,⁹ Y. Watanabe,¹⁴ R. Wedd,²⁰ J. Wicht,¹⁷ E. Won,¹⁵ B. D. Yabsley,³⁷ Y. Yamashita,²⁷ M. Yamauchi,⁸ C. Z. Yuan,⁹ Y. Yusa,⁴⁴ C. C. Zhang,⁹ Z. P. Zhang,³⁴ and A. Zupanc¹³

(The Belle Collaboration)

¹*Budker Institute of Nuclear Physics, Novosibirsk*

²*Chiba University, Chiba*

³*University of Cincinnati, Cincinnati, Ohio 45221*

⁴*Justus-Liebig-Universität Gießen, Gießen*

⁵*The Graduate University for Advanced Studies, Hayama*

⁶*Hanyang University, Seoul*

⁷*University of Hawaii, Honolulu, Hawaii 96822*

⁸*High Energy Accelerator Research Organization (KEK), Tsukuba*

⁹*Institute of High Energy Physics, Chinese Academy of Sciences, Beijing*

¹⁰*Institute of High Energy Physics, Vienna*

¹¹*Institute of High Energy Physics, Protvino*

¹²*Institute for Theoretical and Experimental Physics, Moscow*

¹³*J. Stefan Institute, Ljubljana*

¹⁴*Kanagawa University, Yokohama*

¹⁵*Korea University, Seoul*

¹⁶*Kyungpook National University, Taegu*

¹⁷*École Polytechnique Fédérale de Lausanne (EPFL), Lausanne*

¹⁸*Faculty of Mathematics and Physics, University of Ljubljana, Ljubljana*

¹⁹*University of Maribor, Maribor*

²⁰*University of Melbourne, School of Physics, Victoria 3010*

²¹*Nagoya University, Nagoya*

²²*Nara Women's University, Nara*

²³*National Central University, Chung-li*

²⁴*National United University, Miao Li*

²⁵*Department of Physics, National Taiwan University, Taipei*

²⁶*H. Niewodniczanski Institute of Nuclear Physics, Krakow*

²⁷*Nippon Dental University, Niigata*

²⁸*Niigata University, Niigata*

²⁹*University of Nova Gorica, Nova Gorica*

³⁰*Osaka City University, Osaka*

³¹*Osaka University, Osaka*

³²*Panjab University, Chandigarh*

³³*Saga University, Saga*

³⁴*University of Science and Technology of China, Hefei*

³⁵Seoul National University, Seoul

³⁶Sungkyunkwan University, Suwon

³⁷University of Sydney, Sydney, New South Wales

³⁸Toho University, Funabashi

³⁹Tohoku Gakuin University, Tagajo

⁴⁰Department of Physics, University of Tokyo, Tokyo

⁴¹Tokyo Institute of Technology, Tokyo

⁴²Tokyo Metropolitan University, Tokyo

⁴³Tokyo University of Agriculture and Technology, Tokyo

⁴⁴Virginia Polytechnic Institute and State University, Blacksburg, Virginia 24061

⁴⁵Yonsei University, Seoul

We report the first observation of $e^+e^- \rightarrow \Upsilon(1S)\pi^+\pi^-$, $\Upsilon(2S)\pi^+\pi^-$, and first evidence for $e^+e^- \rightarrow \Upsilon(3S)\pi^+\pi^-$, $\Upsilon(1S)K^+K^-$, near the peak of the $\Upsilon(5S)$ resonance at $\sqrt{s} \sim 10.87$ GeV. The results are based on a data sample of 21.7 fb^{-1} collected with the Belle detector at the KEKB e^+e^- collider. Attributing the signals to the $\Upsilon(5S)$ resonance, the partial widths $\Gamma(\Upsilon(5S) \rightarrow \Upsilon(1S)\pi^+\pi^-) = 0.59 \pm 0.04(\text{stat}) \pm 0.09(\text{syst}) \text{ MeV}$ and $\Gamma(\Upsilon(5S) \rightarrow \Upsilon(2S)\pi^+\pi^-) = 0.85 \pm 0.07(\text{stat}) \pm 0.16(\text{syst}) \text{ MeV}$ are obtained from the observed cross sections. These values exceed by more than two orders of magnitude the previously measured partial widths for dipion transitions between lower Υ resonances.

PACS numbers: 13.25.Gv, 14.40.Gx

Heavy quarkonia provide a unique nonrelativistic system in which low energy QCD may be illuminated through their energy levels, widths, and transition amplitudes. Dipion transitions between ψ and Υ levels below the open flavor thresholds have been successfully described in terms of multipole moments of the QCD field [1]. The first measurements above the open beauty threshold, namely of $\Upsilon(4S) \rightarrow \Upsilon(1S)\pi^+\pi^-$ [2, 3, 4], are consistent with this picture [5]. (The $\Upsilon(4S)$ is the third radial excitation of the $J^{PC} = 1^{--}$ state $\Upsilon(1S)$.)

The spectroscopy above open flavor threshold is complex, however, as there is no positronium analogue. The recent discovery of a broad 1^{--} state, the $Y(4260)$, decaying with an unexpectedly large partial width to $J/\psi\pi^+\pi^-$ [6], has brought new challenges to the interpretation of its composition, with “hybrid” $c\bar{c}g$ (where g is a gluon) and $c\bar{c}q\bar{q}$ (where $q\bar{q}$ is a color-octet light quark pair) four quark state as possibilities. The observation of a bottomonium counterpart to $Y(4260)$, which we shall refer to as Y_b [7], could shed further light on the structure of such particles. The expected mass is above the $\Upsilon(4S)$. It has been suggested that a Y_b with lower mass can be searched for by radiative return from the $\Upsilon(5S)$, and one with higher mass through an anomalous rate of $\Upsilon(nS)\pi\pi$ events [7]; scaling from $\Upsilon(4S) \rightarrow \Upsilon(1S)\pi\pi$, one expects $\Upsilon(5S) \rightarrow \Upsilon(1S)\pi\pi$ to have branching fraction $\sim 10^{-5}$.

Here we report the first observation of $\Upsilon(1S)\pi^+\pi^-$ and $\Upsilon(2S)\pi^+\pi^-$ final states, as well as evidence for $\Upsilon(3S)\pi^+\pi^-$ and $\Upsilon(1S)K^+K^-$ in a 21.7 fb^{-1} data sample collected near the peak of the $\Upsilon(5S)$ resonance with the Belle detector at the KEKB e^+e^- energy-asymmetric collider [8]. The rates for $\Upsilon(1S)\pi^+\pi^-$ and $\Upsilon(2S)\pi^+\pi^-$ are much larger than the expectations from scaling the comparable $\Upsilon(4S)$ decays to the $\Upsilon(5S)$. Since only one center-of-mass (CM) energy is used, one does not know

whether these enhancements are an effect of the $\Upsilon(5S)$ itself, or due to a nearby or overlapping “ Y_b ” state. Throughout this Letter, we shall therefore use the notation $\Upsilon(10860)$ instead of $\Upsilon(5S)$.

The Belle detector is a large-solid-angle magnetic spectrometer, which consists of a silicon vertex detector (SVD), a central drift chamber (CDC), an array of aerogel threshold Cherenkov counters (ACC), a barrel-like arrangement of time-of-flight scintillation counters (TOF), and an electromagnetic calorimeter comprised of CsI(Tl) crystals (ECL) located inside a superconducting solenoid that provides a 1.5 T magnetic field. An iron flux-return located outside the coil is instrumented to detect K_L^0 mesons and to identify muons (KLM). The detector is described in detail elsewhere [9].

The $\Upsilon(10860) \rightarrow \Upsilon(nS)\pi^+\pi^-$ and $\Upsilon(1S)K^+K^-$ final states are reconstructed using $\Upsilon(nS) \rightarrow \mu^+\mu^-$ decays. Events with exactly four well-constrained charged tracks and zero net charge are selected. Muon candidates are required to have hits in the KLM detector associated with the extrapolated trajectory of the charged track. Two muons with opposite charge are selected to form a $\Upsilon(nS)$ candidate. The two remaining tracks are treated as pion or kaon candidates. To suppress the background from $\mu^+\mu^-\gamma \rightarrow \mu^+\mu^-e^+e^-$ with photon conversion, pion candidates with positive electron identification are rejected. Electron identification is based on associating the ECL shower energy to the track momentum, dE/dx from CDC, and the ACC response. Kaon candidates are required to have a kaon likelihood, estimated with information from the ACC, TOF, and dE/dx from the CDC, greater than 0.1. This requirement has an efficiency of 98.2%. The cosine of the opening angle between the π^+ and π^- (K^+ and K^-) momenta in the laboratory frame is required to be less than 0.95. The trigger efficiency is

found to be very close to 100% for these final states. To reject (radiative) Bhabha and μ -pair backgrounds, the data are required to satisfy either $\theta_{\max} < 175^\circ$, or $2 \text{ GeV} < \sum E_{\text{ECL}} < 10 \text{ GeV}$, where θ_{\max} is the maximum opening angle between any charged tracks in the CM frame, and $\sum E_{\text{ECL}}$ is the sum of the ECL clusters' energy.

The signal candidates are identified using the kinematic variable ΔM , defined as the difference between $M(\mu^+\mu^-\pi^+\pi^-)$ or $M(\mu^+\mu^-K^+K^-)$ and $M(\mu^+\mu^-)$ for pion or kaon modes. Sharp peaks are expected at $\Delta M = M_{\Upsilon(mS)} - M_{\Upsilon(nS)}$ for $m > n$. For $\Upsilon(10860) \rightarrow \Upsilon(nS)\pi^+\pi^-$ and $\Upsilon(1S)K^+K^-$, signal events should be concentrated at $\Delta M = \sqrt{s} - M_{\Upsilon(nS)}$, since a single CM energy is used.

Figure 1 shows the two-dimensional scatter plot of $M(\mu^+\mu^-)$ vs. ΔM for the data. Clear enhancements are observed, especially for $\Upsilon(10860) \rightarrow \Upsilon(1S)\pi^+\pi^-$ and $\Upsilon(2S)\pi^+\pi^-$ decays. The dominant background processes, $e^+e^- \rightarrow \mu^+\mu^-\gamma$ ($\rightarrow e^+e^-$) and $e^+e^- \rightarrow \mu^+\mu^-\pi^+\pi^-$ accumulate at the kinematic boundary, $M(\mu^+\mu^-\pi^+\pi^-) = \sqrt{s}$. The events with $|M(\mu^+\mu^-\pi^+\pi^-) - \sqrt{s}| < 150 \text{ MeV}$ or $|M(\mu^+\mu^-K^+K^-) - \sqrt{s}| < 150 \text{ MeV}$ are selected. The fitting regions are defined by $1.25 \text{ GeV}/c^2 < \Delta M <$

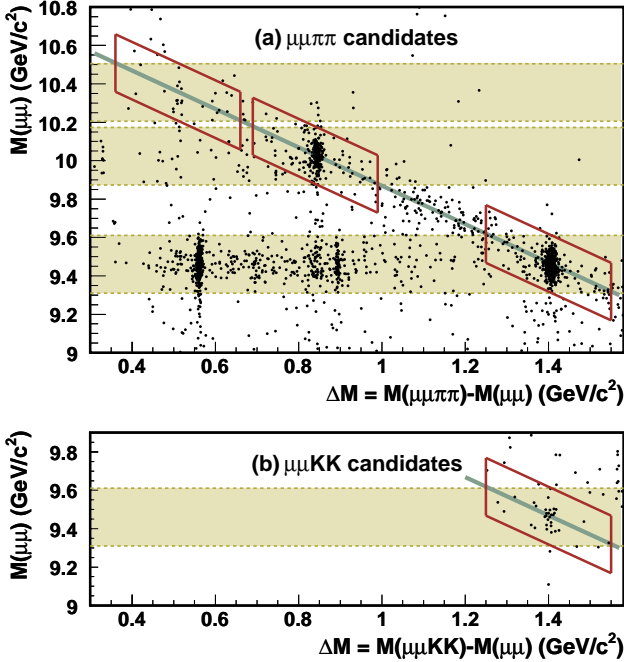


FIG. 1: Scatter plot of $M(\mu^+\mu^-)$ vs. ΔM for the data collected at $\sqrt{s} \sim 10.87 \text{ GeV}$, for (a) $\mu^+\mu^-\pi^+\pi^-$ and (b) $\mu^+\mu^-K^+K^-$ candidates. Horizontal shaded bands correspond to $\Upsilon(1S)$, $\Upsilon(2S)$ and $\Upsilon(3S)$ (only $\Upsilon(1S)$ for (b)), and open boxes are the fitting regions for $\Upsilon(10860) \rightarrow \Upsilon(nS)\pi^+\pi^-$ and $\Upsilon(1S)K^+K^-$. The lines indicate the kinematic boundaries, $M(\mu^+\mu^-\pi^+\pi^-), \mu^+\mu^-K^+K^- = \sqrt{s}$.

$1.55 \text{ GeV}/c^2$, $0.69 \text{ GeV}/c^2 < \Delta M < 0.99 \text{ GeV}/c^2$, and $0.36 \text{ GeV}/c^2 < \Delta M < 0.66 \text{ GeV}/c^2$ for $\Upsilon(10860) \rightarrow \Upsilon(1S)\pi^+\pi^-$, $\Upsilon(2S)\pi^+\pi^-$, and $\Upsilon(3S)\pi^+\pi^-$, respectively. The fitting region in ΔM for $\Upsilon(10860) \rightarrow \Upsilon(1S)K^+K^-$ is the same as for the $\Upsilon(1S)\pi^+\pi^-$ mode. The oblique fitting regions are selected so that the background shape is monotonic along each band. The background distributions are verified using the off-resonance sample (recorded at $\sqrt{s} \sim 10.52 \text{ GeV}$) [4].

The ΔM distributions for the $\mu^+\mu^-\pi^+\pi^-$ candidates in the $\Upsilon(1S)$ and $\Upsilon(2S) \rightarrow \mu^+\mu^-$ mass bands are shown in Fig. 2. The peaks for $\Upsilon(10860) \rightarrow \Upsilon(1S)\pi^+\pi^-$ and $\Upsilon(2S)\pi^+\pi^-$ are located at $\Delta M \sim 1.41 \text{ GeV}/c^2$ and $\sim 0.84 \text{ GeV}/c^2$, respectively. Two other peaks at $\Delta M \sim 0.56 \text{ GeV}/c^2$ and $\sim 0.89 \text{ GeV}/c^2$ correspond to $\Upsilon(2S) \rightarrow \Upsilon(1S)\pi^+\pi^-$ and $\Upsilon(3S) \rightarrow \Upsilon(1S)\pi^+\pi^-$ transitions, respectively. The absence of a peak around $1.12 \text{ GeV}/c^2$ corresponding to $\Upsilon(4S) \rightarrow \Upsilon(1S)\pi^+\pi^-$ is consistent with the rates measured in Refs. [3, 4]. The structure just below $\Upsilon(3S) \rightarrow \Upsilon(1S)\pi^+\pi^-$ in the ΔM distribution is from the cascade decays $\Upsilon(10860) \rightarrow \Upsilon(2S)\pi^+\pi^-$ with $\Upsilon(2S) \rightarrow \Upsilon(1S)[\rightarrow \mu^+\mu^-]X$.

Signal yields are extracted by unbinned extended maximum likelihood (ML) fits to the ΔM distributions. The likelihood for the fit is written as

$$\mathcal{L}(N_s, N_b) = \frac{e^{-(N_s+N_b)}}{N!} \prod_{i=1}^N [N_s \cdot P_s(\Delta M_i) + N_b \cdot P_b(\Delta M_i)], \quad (1)$$

where N_s (N_b) denotes the yield for signal (background), and P_s (P_b) is the signal (background) probability density function (PDF). The signal is described by a sum of two Gaussians while the background is approximated by a linear function. The tail part of the signal PDF is parameterized by a broad Gaussian, whose width and frac-

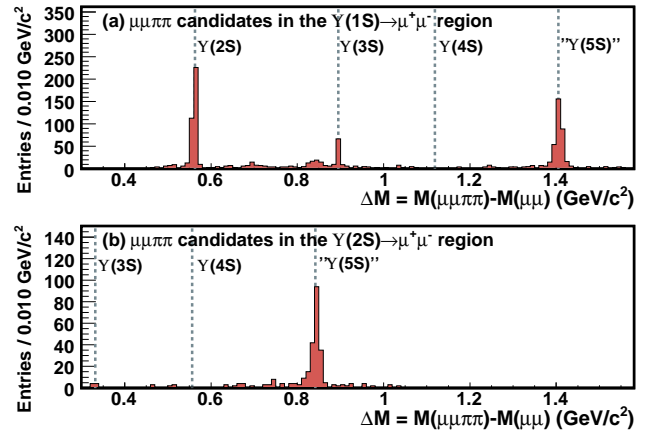


FIG. 2: The ΔM distributions for $\mu^+\mu^-\pi^+\pi^-$ events in the (a) $\Upsilon(1S) \rightarrow \mu^+\mu^-$ and (b) $\Upsilon(2S) \rightarrow \mu^+\mu^-$ bands of Fig. 1(a). Vertical dashed lines show the expected ΔM values for the $\Upsilon(nS) \rightarrow \Upsilon(1,2S)\pi^+\pi^-$ transitions.

tion (of area) are fixed from Monte Carlo (MC) simulation. For the $\Upsilon(10860) \rightarrow \Upsilon(1S)\pi^+\pi^-$ and $\Upsilon(2S)\pi^+\pi^-$ modes, the remaining PDF parameters and yields of signal and background are floated in the fits. For the $\Upsilon(10860) \rightarrow \Upsilon(3S)\pi^+\pi^-$ and $\Upsilon(1S)K^+K^-$ transitions, where statistics are limited, the means and widths are established based on $\Upsilon(10860) \rightarrow \Upsilon(1S)\pi^+\pi^-$ events and fixed in the fits. We observe 325^{+20}_{-19} , 186 ± 15 , $10.5^{+4.0}_{-3.3}$, and $20.2^{+5.2}_{-4.5}$ events in the $\Upsilon(10860) \rightarrow \Upsilon(1S)\pi^+\pi^-$, $\Upsilon(2S)\pi^+\pi^-$, $\Upsilon(3S)\pi^+\pi^-$, and $\Upsilon(1S)K^+K^-$ channels, with significances of 20σ , 14σ , 3.2σ , and 4.9σ , respectively. The significance is calculated using the difference in likelihood values of the best fit and of a null signal hypothesis including the effect of systematic uncertainties. The Gaussian widths of the $\Upsilon(10860) \rightarrow \Upsilon(1S)\pi^+\pi^-$ and $\Upsilon(2S)\pi^+\pi^-$ peaks are found to be 8.0 ± 0.5 MeV/ c^2 and 7.6 ± 0.7 MeV/ c^2 , respectively, and are consistent with the MC predictions. The distributions of ΔM with the fit results superimposed are shown in Fig. 3.

The yields for $\Upsilon(10860) \rightarrow \Upsilon(1S)\pi^+\pi^-$, $\Upsilon(2S)\pi^+\pi^-$ are found to be large; thus, the corresponding invariant masses of the $\pi^+\pi^-$ system, $M(\pi^+\pi^-)$, and the cosine of the helicity angle, $\cos\theta_{\text{Hel}}$, can be examined in detail. The helicity angle, θ_{Hel} , is the angle between the π^- and $\Upsilon(10860)$ momenta in the $\pi^+\pi^-$ rest frame. Figure 4 shows the $\Upsilon(10860)$ yields as functions of $M(\pi^+\pi^-)$ and $\cos\theta_{\text{Hel}}$, which are extracted using ML fits to ΔM in bins of $M(\pi^+\pi^-)$ or $\cos\theta_{\text{Hel}}$. The shaded histograms in the figure are the distributions from MC simulations using the model of Ref. [1], while the open histograms show a generic phase space model. As neither model agrees well with the observed distributions and the efficiencies are sensitive to both variables, the reconstruction efficiencies for $\Upsilon(10860) \rightarrow \Upsilon(1S)\pi^+\pi^-$ and $\Upsilon(2S)\pi^+\pi^-$ are obtained using MC samples reweighted according to the measured $M(\pi^+\pi^-)$ and $\cos\theta_{\text{Hel}}$ spectra. Due to limited statistics, we estimate the reconstruction efficiencies for $\Upsilon(10860) \rightarrow \Upsilon(3S)\pi^+\pi^-$ and $\Upsilon(1S)K^+K^-$ modes using the model of Ref. [1]. Comparison of the $M(\pi^+\pi^-)$ distribution obtained here with other $\Upsilon(nS) \rightarrow \Upsilon(mS)\pi^+\pi^-$ ($m < n$) decays could be important for the theoretical interpretation of the results [1, 5].

Assuming that signal events come only from the $\Upsilon(5S)$ resonance, the corresponding branching fractions and partial widths can be extracted using ratios to the $\Upsilon(5S)$ cross section at $\sqrt{s} \sim 10.87$ GeV, 0.302 ± 0.015 nb [11]. The results, including the observed cross sections, are given in Table I. The values include the world average branching fractions for $\Upsilon(nS) \rightarrow \mu^+\mu^-$ decays, and the total width of the $\Upsilon(5S)$ [10]. The measured partial widths, of order 0.6–0.8 MeV, are large compared to all other known transitions among $\Upsilon(nS)$ states. The partial widths for $\Upsilon(2S)$, $\Upsilon(3S)$, and $\Upsilon(4S) \rightarrow \Upsilon(1S)\pi^+\pi^-$ transitions are all at the keV level (Table II).

The systematic uncertainties for the cross sections are dominated by the $\Upsilon(nS) \rightarrow \mu^+\mu^-$ branching frac-

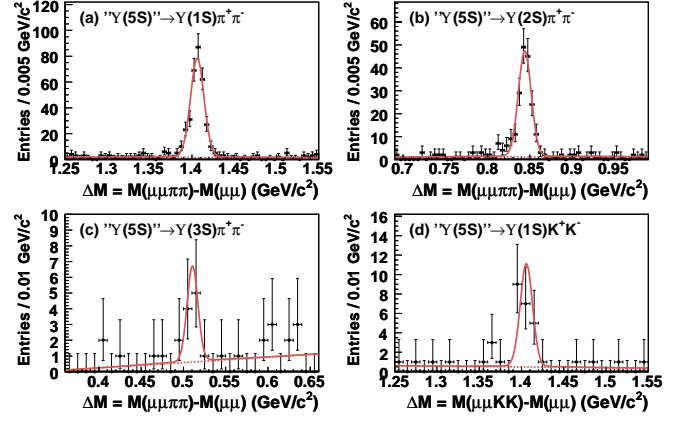


FIG. 3: The ΔM distributions for (a) $\Upsilon(1S)\pi^+\pi^-$, (b) $\Upsilon(2S)\pi^+\pi^-$, (c) $\Upsilon(3S)\pi^+\pi^-$, and (d) $\Upsilon(1S)K^+K^-$ with the fit results superimposed. The dashed curves show the background components in the fits.

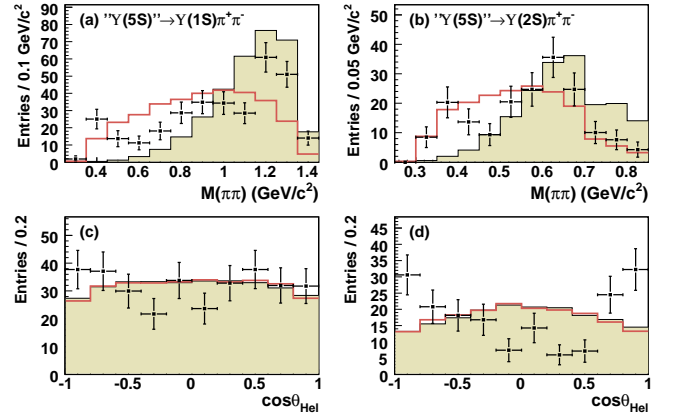


FIG. 4: The $\Upsilon(10860)$ yields as functions of $M(\pi^+\pi^-)$ and $\cos\theta_{\text{Hel}}$ for (a,c) $\Upsilon(1S)\pi^+\pi^-$ and (b,d) $\Upsilon(2S)\pi^+\pi^-$ transitions. The shaded (open) histogram are from MC simulations using the model of Ref. [1] (phase space model). The numerical yields are given in the appendix.

tions, MC reconstruction efficiencies, and PDF parameterization for the fits. Uncertainties of 2.0%, 8.8%, and 9.6% for the $\Upsilon(1S)$, $\Upsilon(2S)$, and $\Upsilon(3S) \rightarrow \mu^+\mu^-$ branching fractions are included, respectively. For the $\Upsilon(1S)\pi^+\pi^-$ and $\Upsilon(2S)\pi^+\pi^-$ modes, the reconstruction efficiencies are obtained from MC simulations using the observed $M(\pi^+\pi^-)$ and $\cos\theta_{\text{Hel}}$ distributions as inputs. The uncertainties associated with these distributions give rise to 4.4% and 6.8% errors for the $\Upsilon(1S)\pi^+\pi^-$ and $\Upsilon(2S)\pi^+\pi^-$ MC efficiencies, respectively. For the other two channels, we try as input the models of Ref. [1] and phase space model; the corresponding variations in acceptance are included as systematic uncertainties. A relatively large uncertainty of 13.6% arises for the $\Upsilon(10860) \rightarrow \Upsilon(1S)K^+K^-$ channel, while the corre-

TABLE I: Signal yield (N_s), significance (Σ), reconstruction efficiency, and observed cross section (σ) for $e^+e^- \rightarrow \Upsilon(nS)\pi^+\pi^-$ and $\Upsilon(1S)K^+K^-$ at $\sqrt{s} \sim 10.87$ GeV. Assuming the $\Upsilon(5S)$ to be the sole source of the observed events, the branching fractions (\mathcal{B}) and the partial widths (Γ) for $\Upsilon(5S) \rightarrow \Upsilon(nS)\pi^+\pi^-$ and $\Upsilon(1S)K^+K^-$ are also given. The first uncertainty is statistical, and the second is systematic.

Process	N_s	Σ	Eff.(%)	$\sigma(\text{pb})$	$\mathcal{B}(\%)$	$\Gamma(\text{MeV})$
$\Upsilon(1S)\pi^+\pi^-$	325^{+20}_{-19}	20σ	37.4	$1.61 \pm 0.10 \pm 0.12$	$0.53 \pm 0.03 \pm 0.05$	$0.59 \pm 0.04 \pm 0.09$
$\Upsilon(2S)\pi^+\pi^-$	186 ± 15	14σ	18.9	$2.35 \pm 0.19 \pm 0.32$	$0.78 \pm 0.06 \pm 0.11$	$0.85 \pm 0.07 \pm 0.16$
$\Upsilon(3S)\pi^+\pi^-$	$10.5^{+4.0}_{-3.3}$	3.2σ	1.5	$1.44^{+0.55}_{-0.45} \pm 0.19$	$0.48^{+0.18}_{-0.15} \pm 0.07$	$0.52^{+0.20}_{-0.17} \pm 0.10$
$\Upsilon(1S)K^+K^-$	$20.2^{+5.2}_{-4.5}$	4.9σ	20.3	$0.185^{+0.048}_{-0.041} \pm 0.028$	$0.061^{+0.016}_{-0.014} \pm 0.010$	$0.067^{+0.017}_{-0.015} \pm 0.013$

TABLE II: The total width Γ_{total} , and the partial width $\Gamma_{e^+e^-}$, $\Gamma_{\Upsilon(1S)\pi^+\pi^-}$. Most values are from Refs. [3, 4, 10].

Process	Γ_{total}	$\Gamma_{e^+e^-}$	$\Gamma_{\Upsilon(1S)\pi^+\pi^-}$
$\Upsilon(2S) \rightarrow \Upsilon(1S)\pi^+\pi^-$	0.032 MeV	0.612 keV	0.0060 MeV
$\Upsilon(3S) \rightarrow \Upsilon(1S)\pi^+\pi^-$	0.020 MeV	0.443 keV	0.0009 MeV
$\Upsilon(4S) \rightarrow \Upsilon(1S)\pi^+\pi^-$	20.5 MeV	0.272 keV	0.0019 MeV
$\Upsilon(10860) \rightarrow \Upsilon(1S)\pi^+\pi^-$	110 MeV	0.31 keV	0.59 MeV

sponding error for $\Upsilon(10860) \rightarrow \Upsilon(3S)\pi^+\pi^-$ is small (3.2%) due to the limited phase space. The uncertainties from PDF parameterization are obtained either by replacing the signal PDF with a sum of three Gaussians, or by replacing the background PDF with a second-order polynomial. The differences between the fit results obtained with alternative PDFs and the nominal results are taken as the systematic uncertainty. The selection criteria for rejecting radiative Bhabha and μ -pair events are examined using the data [12] collected at the $\Upsilon(3S)$ resonance. The 1.9% difference between data and MC efficiencies for $\Upsilon(3S) \rightarrow \Upsilon(1S)\pi^+\pi^-$ decays is included as a systematic uncertainty. Other uncertainties included are: tracking efficiency (1% per charged track), muon identification (0.5% per muon candidate), electron rejection for the charged pions (0.1–0.2% per pion), kaon identification (1.8% per kaon), trigger efficiencies (0.9–4.5%), and KEKB luminosity (1.4%). The uncertainties from all sources are added in quadrature. The total systematic uncertainties are 7.5%, 13.5%, 13.1%, and 15.3% for the $\Upsilon(1S)\pi^+\pi^-$, $\Upsilon(2S)\pi^+\pi^-$, $\Upsilon(3S)\pi^+\pi^-$, and $\Upsilon(1S)K^+K^-$ channels, respectively.

For branching fraction estimation, the error in the $\Upsilon(5S)$ cross section (± 0.015 nb) gives a 5.0% uncertainty in signal normalization. For the partial widths, there is an additional uncertainty of 11.8% coming from using the total width of the $\Upsilon(5S)$.

In summary, we report the first observation of $e^+e^- \rightarrow \Upsilon(1S)\pi^+\pi^-$ and $\Upsilon(2S)\pi^+\pi^-$ transitions, and first evidence of $e^+e^- \rightarrow \Upsilon(3S)\pi^+\pi^-$ and $\Upsilon(1S)K^+K^-$ transitions at a CM energy near the $\Upsilon(5S)$ resonance of $\sqrt{s} \sim$

10.87 GeV. Clear signals are observed at the expected CM energy, with subsequent $\Upsilon(nS) \rightarrow \mu^+\mu^-$ decay. The measured cross sections are $1.61 \pm 0.10 \pm 0.12$ pb, $2.35 \pm 0.19 \pm 0.32$ pb, $1.44^{+0.55}_{-0.45} \pm 0.19$ pb, and $0.185^{+0.048}_{-0.041} \pm 0.028$ pb for $e^+e^- \rightarrow \Upsilon(1S)\pi^+\pi^-$, $\Upsilon(2S)\pi^+\pi^-$, $\Upsilon(3S)\pi^+\pi^-$, and $\Upsilon(1S)K^+K^-$ transitions, respectively. The first uncertainty is statistical, and the second is systematic. Assuming the observed signal events are due solely to the $\Upsilon(5S)$ resonance, branching fractions are measured to be in the range (0.48–0.78)% for $\Upsilon(nS)\pi^+\pi^-$ channels, and 0.061% for the $\Upsilon(1S)K^+K^-$ channel. The corresponding partial widths are found to be in the range (0.52–0.85) MeV for $\Upsilon(nS)\pi^+\pi^-$, and 0.067 MeV for the $\Upsilon(1S)K^+K^-$ mode, more than two orders of magnitude larger than the corresponding partial widths for $\Upsilon(4S)$, $\Upsilon(3S)$ or $\Upsilon(2S)$ decays. The unexpectedly large partial widths disagree with the expectation for a pure $b\bar{b}$ state, unless there is a new mechanism to enhance the decay rate. A detailed energy scan within the $\Upsilon(5S)$ energy region would help to extract the resonant spectrum; a comparison between the yield of $\Upsilon(nS)\pi^+\pi^-$ events and the total hadronic cross section may help us to understand the nature of the signal.

We thank the KEKB group for excellent operation of the accelerator, the KEK cryogenics group for efficient solenoid operations, and the KEK computer group and the NII for valuable computing and Super-SINET network support. We acknowledge support from MEXT and JSPS (Japan); ARC and DEST (Australia); NSFC (China); DST (India); MOEHRD, KOSEF, KRF and SBS Foundation (Korea); KBN (Poland); MES and RFAAE (Russia); ARRS (Slovenia); SNSF (Switzerland); NSC and MOE (Taiwan); and DOE (USA).

-
- [1] L. S. Brown and R. N. Cahn, Phys. Rev. Lett. **35**, 1 (1975); M. B. Voloshin, JETP Lett. **21**, 347 (1975); Y. P. Kuang and T. M. Yan, Phys. Rev. D **24**, 2874 (1981).
 - [2] F. Butler *et al.* [CLEO Collaboration], Phys. Rev. D **49**, 40 (1994); D. Cronin-Hennessy *et al.* [CLEO Collaboration], Phys. Rev. D **76**, 072001 (2007).

- [3] B. Aubert *et al.* [BaBar Collaboration], Phys. Rev. Lett. **96**, 232001 (2006).
- [4] A. Sokolov *et al.* [Belle Collaboration], Phys. Rev. D **75**, 071103 (2007).
- [5] Yu. A. Simonov, JETP Lett. **87**, 147 (2008).
- [6] B. Aubert *et al.* [BaBar Collaboration], Phys. Rev. Lett. **95**, 142001 (2005).
- [7] W. S. Hou, Phys. Rev. D **74**, 017504 (2006).
- [8] S. Kurokawa and E. Kikutani, Nucl. Instrum. Methods Phys. Res., Sect. A **499**, 1 (2003), and other papers included in this Volume.
- [9] A. Abashian *et al.* [Belle Collaboration], Nucl. Instrum. Methods Phys. Res., Sect. A **479**, 117 (2002).
- [10] W.-M. Yao *et al.*, J. Phys. G **33**, 1 (2006).
- [11] A. Drutskoy *et al.* [Belle Collaboration], Phys. Rev. Lett. **98**, 052001 (2007).
- [12] O. Tajima *et al.* [Belle Collaboration], Phys. Rev. Lett. **98**, 132001 (2007).

**APPENDIX: YIELDS OF $\Upsilon(10860) \rightarrow \Upsilon(1S)\pi^+\pi^-$
AND $\Upsilon(2S)\pi^+\pi^-$ TRANSITIONS AS FUNCTIONS
OF $M(\pi^+\pi^-)$ AND $\cos\theta_{\text{Hel}}$**

TABLE III: Numerical yields of $\Upsilon(10860) \rightarrow \Upsilon(1S)\pi^+\pi^-$ and $\Upsilon(2S)\pi^+\pi^-$ transitions as functions of $M(\pi^+\pi^-)$ and $\cos\theta_{\text{Hel}}$ which are shown in Figure 4. The uncertainties of the yields are statistical only.

Bin	$\Upsilon(1S)\pi^+\pi^-$		$\Upsilon(2S)\pi^+\pi^-$	
	$M(\pi^+\pi^-)$ (GeV)	Yield	$M(\pi^+\pi^-)$ (GeV)	Yield
1	[0.25, 0.35)	$1.83^{+1.84}_{-1.16}$	[0.25, 0.30)	0.0
2	[0.35, 0.45)	$25.03^{+5.70}_{-4.97}$	[0.30, 0.35)	$8.48^{+3.51}_{-2.82}$
3	[0.45, 0.55)	$13.67^{+4.66}_{-3.94}$	[0.35, 0.40)	$20.31^{+5.22}_{-4.52}$
4	[0.55, 0.65)	$11.21^{+3.99}_{-3.28}$	[0.40, 0.45)	$13.69^{+4.38}_{-3.70}$
5	[0.65, 0.75)	$18.16^{+5.12}_{-4.41}$	[0.45, 0.50)	$9.37^{+3.73}_{-3.02}$
6	[0.75, 0.85)	$28.70^{+6.18}_{-5.47}$	[0.50, 0.55)	$20.51^{+5.27}_{-4.58}$
7	[0.85, 0.95)	$34.84^{+6.70}_{-5.97}$	[0.55, 0.60)	$24.70^{+5.70}_{-4.97}$
8	[0.95, 1.05)	$34.35^{+6.57}_{-5.86}$	[0.60, 0.65)	$35.58^{+6.83}_{-6.10}$
9	[1.05, 1.15)	$28.49^{+6.03}_{-5.35}$	[0.65, 0.70)	$24.70^{+5.58}_{-4.88}$
10	[1.15, 1.25)	$60.91^{+8.57}_{-7.87}$	[0.70, 0.75)	$10.07^{+3.74}_{-3.03}$
11	[1.25, 1.35)	$50.99^{+7.48}_{-6.81}$	[0.75, 0.80)	$7.60^{+3.35}_{-2.64}$
12	[1.35, 1.45)	$14.00^{+4.09}_{-3.41}$	[0.80, 0.85)	$4.28^{+2.58}_{-1.88}$
Bin	$\cos\theta_{\text{Hel}}$	Yield	$\cos\theta_{\text{Hel}}$	Yield
1	[-1.0, -0.8)	$37.68^{+6.90}_{-6.24}$	[-1.0, -0.8)	$30.59^{+6.15}_{-5.46}$
2	[-0.8, -0.6)	$37.09^{+6.90}_{-6.20}$	[-0.8, -0.6)	$20.82^{+5.14}_{-4.49}$
3	[-0.6, -0.4)	$29.95^{+6.07}_{-5.41}$	[-0.6, -0.4)	$18.15^{+4.83}_{-4.14}$
4	[-0.4, -0.2)	$21.74^{+5.51}_{-4.84}$	[-0.4, -0.2)	$16.78^{+4.78}_{-4.07}$
5	[-0.2, +0.0)	$33.77^{+6.48}_{-5.85}$	[-0.2, +0.0)	$7.45^{+3.53}_{-2.78}$
6	[+0.0, +0.2)	$23.65^{+5.55}_{-4.84}$	[+0.0, +0.2)	$14.28^{+4.53}_{-3.76}$
7	[+0.2, +0.4)	$32.80^{+6.34}_{-5.67}$	[+0.2, +0.4)	$6.00^{+3.07}_{-2.36}$
8	[+0.4, +0.6)	$37.72^{+6.86}_{-6.17}$	[+0.4, +0.6)	$7.15^{+3.44}_{-2.75}$
9	[+0.6, +0.8)	$31.97^{+6.33}_{-5.65}$	[+0.6, +0.8)	$24.49^{+5.65}_{-4.95}$
10	[+0.8, +1.0)	$31.75^{+6.28}_{-5.58}$	[+0.8, +1.0)	$32.26^{+6.41}_{-5.65}$